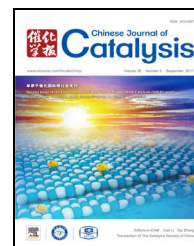


available at www.sciencedirect.comjournal homepage: www.elsevier.com/locate/chnjc

Article (Special Issue of the International Symposium on Single-Atom Catalysis (ISSAC-2016))

Coating Pd/Al₂O₃ catalysts with FeO_x enhances both activity and selectivity in 1,3-butadiene hydrogenation



Hong Yi, Yujia Xia, Huan Yan, Junling Lu*

Department of Chemical Physics, Hefei National Laboratory for Physical Sciences at the Microscale, Collaborative Innovation Center of Chemistry for Energy Materials (iChEM), CAS Key Laboratory of Materials for Energy Conversion, University of Science and Technology of China, Hefei 230026, Anhui, China

ARTICLE INFO

Article history:

Received 26 November 2016

Accepted 30 December 2016

Published 5 September 2017

Keywords:

Palladium catalyst

Atomic layer deposition

Hydrogenation

1,3-Butadiene

Selectivity

Activity

Strong metal support interaction

ABSTRACT

Pd-based catalysts are widely used in hydrogenation reactions, and it is essential to improve the selectivity of these catalysts to give the desired products, especially at high conversions. However, improvements in selectivity have generally been achieved at the expense of catalytic activity. Here, we report that deposition of FeO_x onto a Pd/Al₂O₃ catalyst using atomic layer deposition with precise, near atomic control provides a remarkable improvement in both activity and butene selectivity in the selective hydrogenation of 1,3-butadiene under mild conditions. Diffuse reflectance infrared Fourier transform spectroscopy for CO chemisorption measurements illustrate that FeO_x preferentially nucleates on Pd (111) facets and divides the Pd surface atoms into small ensembles. X-ray photoelectron spectroscopy measurements revealed that the Pd became electron deficient after FeO_x deposition owing to the strong Pd–FeO_x interaction. Our results suggest that a geometric effect, that is, the formation of small Pd ensembles, is the main contributor to the improvement in butene selectivity, whereas the enhancement in hydrogenation activity may be attributed to both electronic effects and the newly generated Pd–FeO_x interface.

© 2017, Dalian Institute of Chemical Physics, Chinese Academy of Sciences.

Published by Elsevier B.V. All rights reserved.

1. Introduction

Alkene streams from industrial naphtha cracking often contain about 1% diene or alkyne side products. The concentrations of these side products must be reduced to less than 10 ppm because they can quickly poison the downstream catalysts used in the polymerization process [1–6]. The selective hydrogenation of 1,3-butadiene to butenes is the most promising way to solve this issue [5], and Pd-based catalysts have been widely used for this purpose owing to their high hydrogenation activity [7–13]. However, Pd monometallic catalysts generally exhibit

low alkene selectivity at high conversions, and are quickly deactivated by heavy coking during reactions.

Extensive efforts have been devoted to the modification of Pd catalysts to improve the butene selectivity and catalyst stability [1,3,7,13–17]. The decoration of Pd with a secondary metal to form bimetallic nanoparticles is a common method, and allows the Pd electronic properties and surface ensembles to be tailored to enhance the selectivity of the catalyst [1,11,13,17–19]. However, improvements in the selectivity have generally been achieved at the expense of catalytic activity. For example, Kolli et al. [10] synthesized a series of

* Corresponding author. Tel: +86-551-63600359; E-mail: junling@ustc.edu.cn

This work was supported by the One Thousand Young Talents Program under the Recruitment Program of Global Experts, the National Natural Science Foundation of China (21673215, 51402283, 21473169), and the Fundamental Research Funds for the Central Universities (WK2060030017), and the Startup Funds from University of Science and Technology of China.

DOI: 10.1016/S1872-2067(17)62768-2 | <http://www.sciencedirect.com/science/journal/18722067> | Chin. J. Catal., Vol. 38, No. 9, September 2017

AuPd/ δ -Al₂O₃ catalysts with different atomic Au/Pd ratios, and found that although increasing the Au/Pd ratio above 15 markedly increased the selectivity, the catalytic activity was considerably decreased. Similarly, Zhang [5] reported that Ag-alloyed Pd single-atom catalysts, which are processed with only ppm levels of Pd, showed excellent ethylene selectivity at high acetylene conversions over a wide temperature range. However, the activity was considerably decreased and 100% conversion was achieved only above 160 °C owing to the extremely low Pd concentration. Recently, Chen and co-workers [19] showed that NiPd/ γ -Al₂O₃ catalysts exhibited both higher 1-butene selectivity and higher hydrogenation activity than the monometallic catalysts. Unfortunately, the improved butene selectivity was only achieved at 1,3-butadiene conversions below 60%.

Applying oxide coatings to Pd catalysts has proved to be another effective way of dividing Pd surface ensembles for selectivity improvement [7,15,17,20,21]. For example, Kang et al. [21] reported that Pd/SiO₂ catalysts coated with TiO_x, NbO_x, or CeO_x exhibited considerably higher ethylene selectivity than uncoated Pd/SiO₂ in acetylene hydrogenation after reduction at 500 °C. Later, they also found that TiO₂-modified Pd/SiO₂ catalysts showed improved selectivity for conversion of 1,3-butadiene to 1-butene, essentially without changing the activity [15]. Furthermore, Crabb et al. [17] reported that addition of FeO_x onto Pd or Pt catalysts could suppress the total hydrogenation to butane to some extent. Nevertheless, the reduction in hydrogenation activity caused by carbon deposition or blocking of the active sites by FeO_x was still severe. In our previous studies, we have shown that deposition of microporous alumina layers with a thickness of approximately 3.8 nm onto Pd/Al₂O₃ catalysts by atomic layer deposition (ALD) not only considerably improved the butene selectivity to close to 100% at 95% 1,3-butadiene conversion, but also exhibited very high stability against coking [7]. The enhanced catalytic performance was attributed to the confinement effect induced by micropores within the ALD alumina layer. We also found that the alumina coating largely blocked the surface Pd active sites, thereby considerably reducing the hydrogenation activity. Recently, we further showed that deposition of Ga₂O₃ on Pd/Al₂O₃ catalysts through ALD could generally enhance ethylene selectivity; however, the activity was very sensitive to the coverage of Ga₂O₃ [20]. Taken together, most studies reported in the literature show that improvement in the alkene selectivity is achieved at the expense of catalytic activity, and there has been very limited success in improving both the activity and selectivity in a Pd-based catalyst system.

ALD is an effective method for catalyst synthesis and post-modification, and has near atomic precision [7,8,22–26]. Herein, we precisely deposited FeO_x onto a Pd/Al₂O₃ catalyst using several cycles of ALD to tune the coverage of FeO_x. We show that decoration of Pd nanoparticles (NPs) with FeO_x remarkably enhanced both hydrogenation activity and butene selectivity in the selective hydrogenation of 1,3-butadiene. The enhanced catalytic performance was attributed to electronic modulation, formation of a Pd–FeO_x interface, and geometric effects.

2. Experimental

2.1. Pd/Al₂O₃ catalyst synthesis

The Pd/Al₂O₃ catalyst was synthesized using a wet-impregnation method [22]. Therein, 0.1 g Pd(NO₃)₂·2H₂O (Aladdin, ≥97.7%) and 0.45 g citric acid (Sinopharm Chemical Reagent Co., Ltd., ≥99.5%) were dissolved in 2.6 mL water to form a Pd–citric acid solution. Then, 4.4 g spherical Al₂O₃ powder (Nanodur, Alfa Aesar, 99.5%) was added and the solution was mixed uniformly. The resulting mixture was dried in an oven at 70 °C for 14 h. Finally, the dried material was calcined in 10% O₂ in He at 400 °C for 2 h, then reduced at 250 °C for 30 min in 10% H₂ in He to obtain the Pd/Al₂O₃ catalyst.

2.2. FeO_x ALD coating

FeO_x ALD was carried out using a viscous flow reactor (GEMSTAR-6™ Benchtop ALD, Arradiance) [7]. Ultra-high-purity N₂ (99.999%) was used as the carrier gas at a flow rate of 200 mL/min. The Pd/Al₂O₃ catalyst was loaded into the ALD reactor, and FeO_x ALD was performed at 150 °C by exposing the sample to alternating cycles of ferrocene and oxygen. The ferrocene precursor was contained in a stainless steel reservoir and heated to 90 °C to achieve a sufficient vapor pressure. The inlet lines were heated to 110 °C to avoid condensation. The time sequence for FeO_x ALD was 300, 200, 500, and 200 s for ferrocene exposure, N₂ purge, O₂ exposure, and N₂ purge, respectively. The resulting Pd/Al₂O₃ samples with different numbers of FeO_x ALD cycles were denoted xFe/Pd/Al₂O₃, where x denotes the number of FeO_x ALD cycles.

2.3. Characterization

The contents of Pd and Fe were determined by inductively coupled plasma atomic emission spectroscopy (ICP-AES) (University of Science and Technology of China). The morphology of the catalysts was characterized on an aberration-corrected high-angle annular dark-field scanning transmission electron microscopy (HAADF-STEM) instrument at 200 kV (JEOL-2010F, University of Science and Technology of China).

Diffuse reflectance infrared Fourier transform spectroscopy (DRIFTS) CO chemisorption measurements were performed on a Nicolet iS10 spectrometer equipped with an MCT detector and a low-temperature reaction cell (Praying Mantis Harrick). After the sample was loaded into the cell, it was first calcined in 10% O₂ in He at 200 °C for 1 h, and this was followed by reduction in 10% H₂ in He at 200 °C for 1 h. The sample was then cooled to room temperature under He and a background spectrum was collected. Subsequently, the sample was exposed to 10% CO in He at a flow rate of 20 mL/min for about 30 min until saturation. Next, the sample was purged with He at a flow rate of 20 mL/min for another 30 min to remove the gas phase CO, and then the DRIFT spectrum was collected with 128 scans at a resolution of 4 cm⁻¹.

X-ray photoelectron spectroscopy (XPS) measurements were obtained on a Thermo-VG scientific Escalab 250 spec-

trometer equipped with an Al anode (Al K_{α} = 1486.6 eV). Before the XPS experiments, all samples were pretreated ex situ at 200 °C in 10% O₂ in Ar for 1 h, then reduced in 10% H₂ in Ar for another 1 h, and finally cooled to room temperature in 10% H₂ in Ar. The samples were then carefully sealed and quickly transferred for the XPS measurements.

2.4. Activity test

Selective hydrogenation of 1,3-butadiene was conducted in a fixed-bed flow reactor. The feed gas consisted of 1.9% 1,3-butadiene, 4.7% H₂, and Ar as the balance gas. The total gas flow rate was maintained at 25 mL/min and 50 mg of each catalyst was used. The catalysts were diluted with 1 g quartz chips (60–80 mesh). Prior to each test, the catalyst was pretreated at 200 °C in 10% O₂ in Ar for 1 h, and then reduced in 10% H₂ in Ar at the same temperature for another 1 h. After the reaction stream was introduced, the catalyst was first stabilized at room temperature for several hours, and then the reaction products were collected and analyzed using an online gas chromatograph equipped with an FID detector and a capillary column (ValcoPLOT VP-Alumina-KCl, 50 m × 0.53 mm).

3. Results and discussion

The Pd and Fe loadings in the $x\text{Fe}/\text{Pd}/\text{Al}_2\text{O}_3$ catalysts were determined by ICP-AES. As shown in Table 1, the Pd loading was 1.0 wt% in all samples, and the Fe loadings were 0.26 wt%, 0.41 wt%, 0.67 wt%, and 0.73 wt% in 6Fe/Pd/Al₂O₃, 10Fe/Pd/Al₂O₃, 20Fe/Pd/Al₂O₃, and 30Fe/Pd/Al₂O₃, respectively. The gradual increase in the Fe loading as a function of the number of FeO_x ALD cycles clearly confirms the successful deposition of FeO_x on the Pd/Al₂O₃ catalyst. Aberration-corrected HAADF-STEM measurements were employed to investigate the morphology of the 30Fe/Pd/Al₂O₃ catalyst. The

Table 1

The Pd and Fe loadings in the $x\text{Fe}/\text{Pd}/\text{Al}_2\text{O}_3$ catalysts determined by ICP-AES.

Sample	Pd loading (wt%)	Fe loading (wt%)
Pd/Al ₂ O ₃	1.0	—
6Fe/Pd/Al ₂ O ₃	1.0	0.26
10Fe/Pd/Al ₂ O ₃	1.0	0.41
20Fe/Pd/Al ₂ O ₃	1.0	0.67
30Fe/Pd/Al ₂ O ₃	1.0	0.73

size of the Pd NPs was on average about 7 nm in this sample, as shown in Fig. 1(a)–(c). Unfortunately, we could not observe the FeO_x layer on the Pd NPs with high resolution STEM (Fig. 1(b)), probably because the FeO_x layer was too thin and therefore showed negligible contrast with the Pd NPs. Nonetheless, elemental mapping using energy-dispersive X-ray spectroscopy (EDS) demonstrated overlapping Pd L_{α} and Fe K_{α} signals, which suggests that the Pd NPs were decorated with FeO_x (Fig. 1(d)–(f)).

Infrared (IR) spectroscopy of CO chemisorbed on Pd NPs has been extensively studied, and the relationship between the IR features and the Pd structure is well established [10,21,22,27]. Here, DRIFTS CO chemisorption measurements were carried out to evaluate the accessibility of Pd NPs after FeO_x deposition. As shown in Fig. 2, the uncoated Pd/Al₂O₃ shows three characteristic peaks at 2083, 1976, and 1942 cm⁻¹, which are assigned to linear CO on corner sites, bridge-bonded CO on edge and step sites, and bridge-bonded CO on (111) facets of Pd NPs, respectively [24]. The intensities of these three CO peaks decreased after application of FeO_x ALD on Pd/Al₂O₃, and, as expected, they further decreased as the number of FeO_x ALD cycles was increased. This result also suggests that the coverage of FeO_x on Pd NPs can be increased gradually with precise control, similar to the trend observed for Al₂O₃ ALD on Pd NPs [7]. In addition, the decrease in the CO peak intensity at

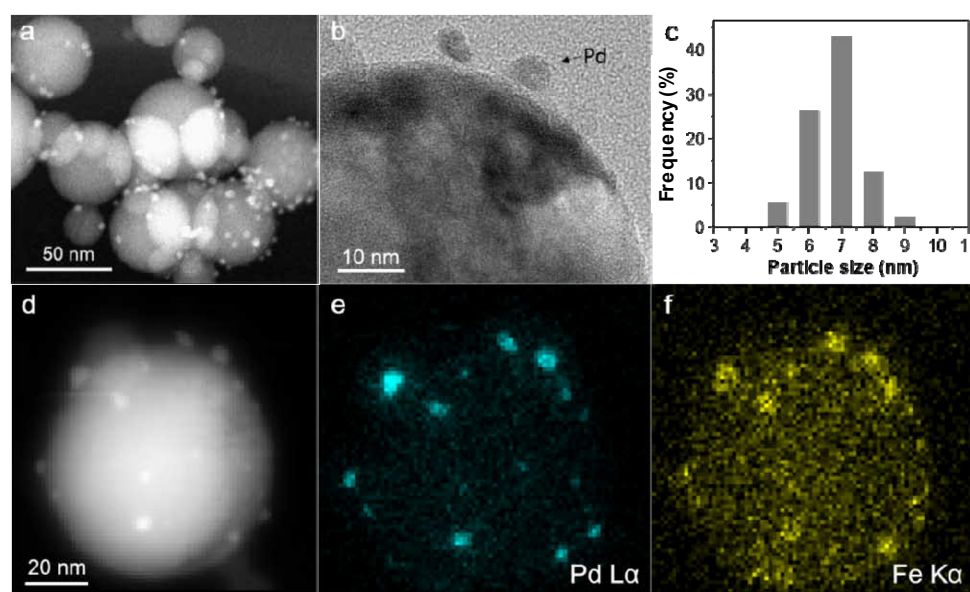


Fig. 1. Representative HAADF-STEM (a) and high-magnification TEM images (b) of the 30Fe/Pd/Al₂O₃ catalyst and the corresponding Pd particle size distribution (c). A HAADF-STEM image (d) of the 30Fe/Pd/Al₂O₃ catalyst, and corresponding EDS mapping of Pd L_{α} (e) and Fe K_{α} signals (f).

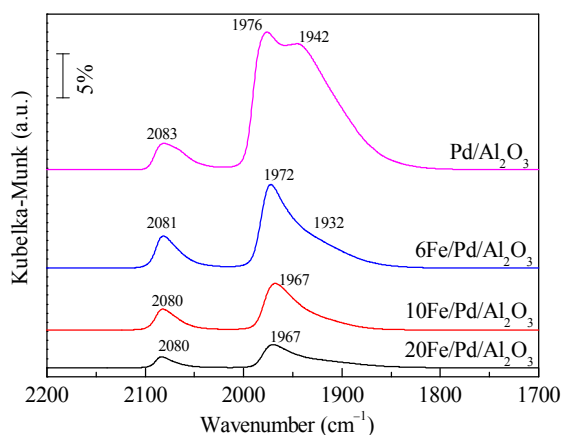


Fig. 2. DRIFT CO chemisorption spectra collected at room temperature on the $x\text{Fe}/\text{Pd}/\text{Al}_2\text{O}_3$ catalysts at the CO saturation coverage. Here $x = 0, 6, 10,$ and $20,$ respectively.

1942 cm⁻¹, assigned to bridge-bonded CO on (111) facets of Pd NPs, was considerably more dramatic than that of the other two CO peaks. This is in contrast to the observed formation of an Al₂O₃ ALD coating on Pd NPs, in which the intensity of bridge-bonded CO on low-coordinate sites decreased more quickly than that of bridge-bonded CO on (111) facet sites [24]. Our result thus implies that FeO_x preferentially decorates the Pd (111) facets and leaves the low-coordinate Pd sites accessible for catalytic function.

The influence of FeO_x on the electronic properties of Pd NPs was investigated by XPS, as shown in Fig. 3. In the Fe 2*p* region (Fig. 3(a)), 6Fe/Pd/Al₂O₃, 10Fe/Pd/Al₂O₃, and 20Fe/Pd/Al₂O₃ showed the same Fe 2*p*_{3/2} binding energy of 710.8 eV, which suggests that the FeO_x species in these samples were mainly in the 3+ oxidation state [28,29]. The increased peak intensities are in line with the increased FeO_x loadings from the increased number of FeO_x ALD cycles (Table 1). In the Pd 3*d* region (Fig. 3(b)), the deconvoluted Pd 3*d*_{5/2} peak at 336.3–336.9 eV in $x\text{Fe}/\text{Pd}/\text{Al}_2\text{O}_3$ ($x = 0, 6, 10, 20$) was assigned to Pd²⁺ [23,30], which implies that the Pd NPs in these samples were partially oxidized as a result of air exposure before the XPS measurements. The deconvoluted Pd 3*d*_{5/2} peak at 335.0 eV in the spec-

trum of uncoated Pd/Al₂O₃ was assigned to metallic Pd [23,30]. After deposition of FeO_x on the Pd/Al₂O₃ catalyst, the Pd 3*d* binding energy of metallic Pd gradually shifted to higher energies and reached 335.4 eV in the spectra of 10Fe/Pd/Al₂O₃ and 20Fe/Pd/Al₂O₃. Clearly, the deposition of FeO_x on Pd NPs resulted in an electron-deficient Pd surface owing to the strong interaction between Pd and FeO_x [31,32]. Interestingly, we also noted that the intensities of the Pd 3*d* XPS peaks in all samples were nearly identical, which implies that the FeO_x film on the Pd NPs was very thin. This is consistent with the low Fe loadings (Table 1) and the STEM observations (Fig. 1(b)).

When the $x\text{Fe}/\text{Pd}/\text{Al}_2\text{O}_3$ catalysts were examined for selective hydrogenation of 1,3-butadiene, all samples were first stabilized in the reaction stream at room temperature. The reaction temperature was then slowly increased to obtain different 1,3-butadiene conversions. As shown in Fig. 4, the 1,3-butadiene conversion was 6.7% on the uncoated Pd/Al₂O₃ catalyst at 25 °C and reached 99% at 43 °C. Surprisingly, all of the Pd/Al₂O₃ samples decorated with FeO_x exhibited considerably higher 1,3-butadiene conversions at room temperature; 30Fe/Pd/Al₂O₃ showed the highest conversion (45%) at 26 °C. However, we did not see an obvious trend in the activity with increasing numbers of FeO_x ALD cycles. Such a remarkable increase in the hydrogenation activity of FeO_x-coated Pd/Al₂O₃ catalysts is rather unusual because the active sites of the Pd NPs were partially blocked by FeO_x, as indicated by the CO chemisorption results in Fig. 2. Indeed, in previous work, we have shown that the microporous Al₂O₃ ALD coating on Pd/Al₂O₃ largely blocks the Pd active sites, thereby considerably reducing the hydrogenation activity [7]. Kang et al. [21] also reported that Pd/SiO₂ catalysts coated with TiO_x, NbO_x, or CeO_x generally exhibited lower activities than uncoated Pd/SiO₂ after reduction at 300 °C in acetylene hydrogenation reactions because the Pd surface of the modified catalysts was partially covered with metal oxides. In addition, these authors observed a negative shift of approximately 0.3 eV in the Pd 3*d* binding energy on metal-oxide-coated Pd/SiO₂ samples. Therefore, an electron-deficient Pd surface, resulting from the strong interaction between Pd and FeO_x, could potentially increase the hydrogenation activity. In contrast, the generated Pd–FeO_x interface may also play an important role in the activity increase

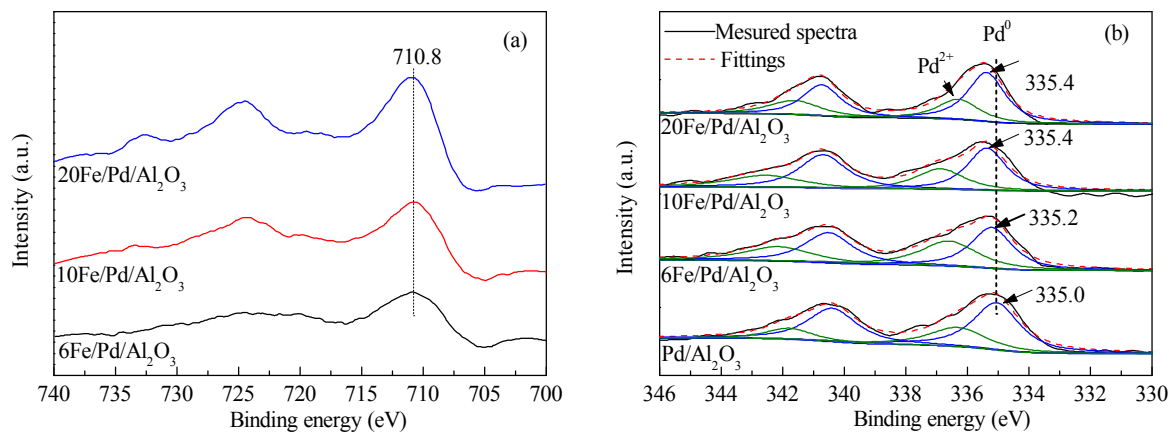


Fig. 3. XPS spectra of the $x\text{Fe}/\text{Pd}/\text{Al}_2\text{O}_3$ catalysts in the Fe 2*p* (a) and Pd 3*d* (b) region.

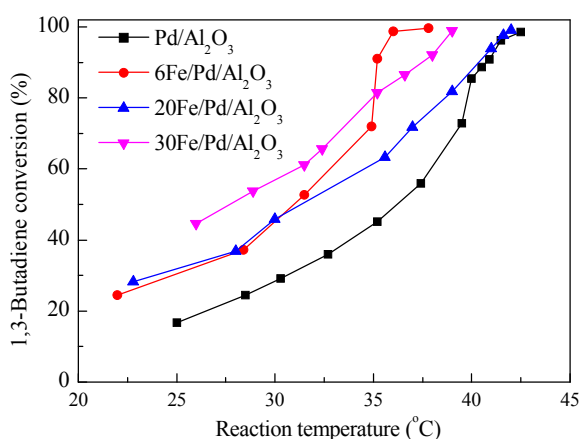


Fig. 4. 1,3-Butadiene conversion as a function of reaction temperature for the $x\text{Fe}/\text{Pd}/\text{Al}_2\text{O}_3$ catalysts. Here $x = 0, 6, 20,$ and 30 , respectively.

[33–36].

The reaction products were plotted as a function of the 1,3-butadiene conversion, as shown in Fig. 5. With the uncoated $\text{Pd}/\text{Al}_2\text{O}_3$ catalyst, the total butene selectivity was 100% below 75% conversion (Fig. 5(a)). The most desired product, 1-butene, was the major product, with a selectivity of 74% (Fig. 5(b)), and the *trans*- and *cis*-2-butene selectivities were 20% and 6%, respectively (Fig. 5(c) and (d)). When the conversion was higher than 75%, the 1-butene selectivity dropped rapidly, and this was accompanied by a sharp increase in butane selectivity. At the same time, the selectivity for *trans*- and *cis*-2-butene first increased slightly at conversions between 75% and 90%, then declined at higher conversions. It is clear

that on increasing the conversion of 1,3-butadiene, secondary hydrogenation of 1-butene to butane occurred first, and secondary hydrogenation of *trans*- and *cis*-2-butene only became pronounced at conversions above 90%. At near complete conversion of 1,3-butadiene (99%), selectivity for butenes decreased to 52%, which is consistent with the previous literature [4,7].

Deposition of FeO_x on $\text{Pd}/\text{Al}_2\text{O}_3$ using ALD caused a slight decrease in the 1-butene selectivity and an increase in the *trans*-2-butene selectivity at low conversions, at which the total butene selectivity was preserved at 100% (Fig. 5(a)–(c)). For example, the selectivity of $30\text{Fe}/\text{Pd}/\text{Al}_2\text{O}_3$ for 1-butene and *trans*-2-butene was about 60% and 35%, respectively, at conversions below 80%. At high 1,3-butadiene conversions (>75%), the total butene selectivity increased dramatically with increasing numbers of FeO_x ALD cycles. The total butene selectivity was about 95% for $30\text{Fe}/\text{Pd}/\text{Al}_2\text{O}_3$ at 99% conversion, which is much higher than that observed for the uncoated $\text{Pd}/\text{Al}_2\text{O}_3$ catalyst (52%). The secondary hydrogenation of all butenes (1-butene, and *trans*- and *cis*-2-butene) to butane was effectively suppressed by the FeO_x coating (Fig. 5(e)). The increase in butene selectivity at high conversions can be mainly attributed to a geometric effect, in which large ensembles of Pd surface atoms were divided into smaller ones by FeO_x ; this is consistent with previous studies [10,15,21,37]. In addition, at conversions above 75%, formation of *trans*- and *cis*-2-butene through isomerization became the dominant secondary reaction on the FeO_x -coated $\text{Pd}/\text{Al}_2\text{O}_3$ catalysts, similar to results seen for the Al_2O_3 ALD-coated Pd catalyst [7]. This change in the reaction pathway, from butene hydrogenation to isomerization, is likely due to the lower concentration of dissociated

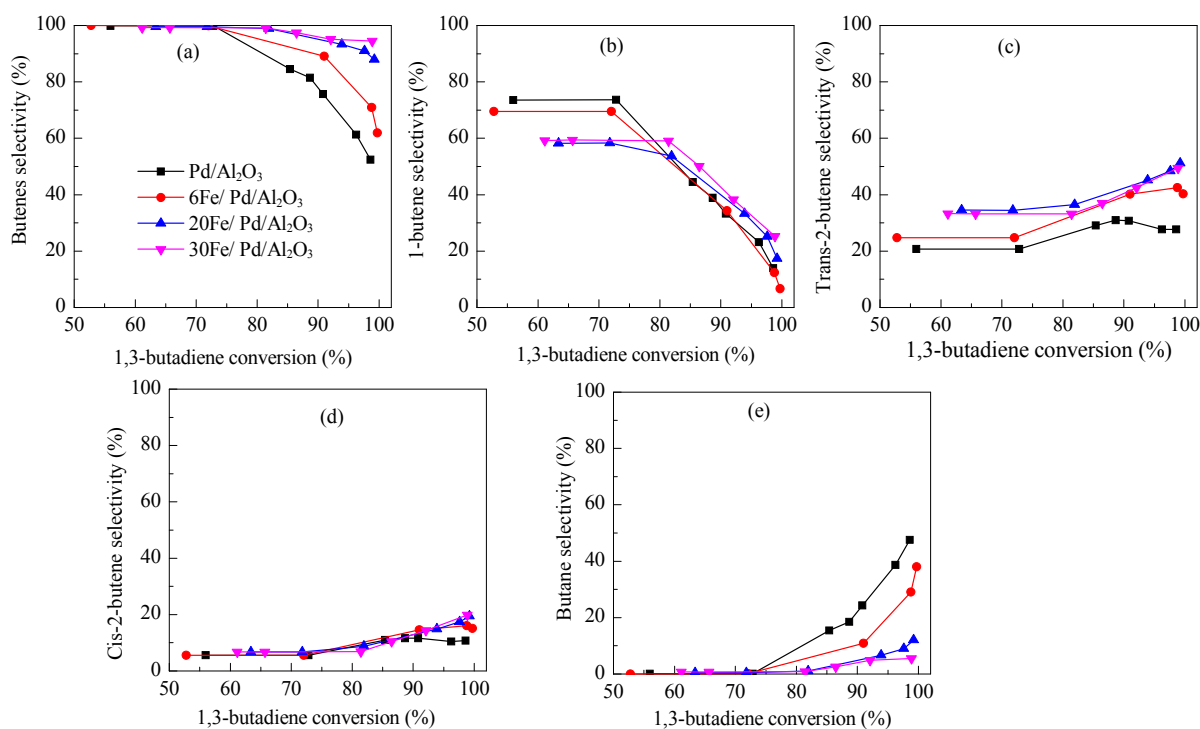


Fig. 5. Product selectivity as a function of 1,3-butadiene conversion over the $x\text{Fe}/\text{Pd}/\text{Al}_2\text{O}_3$ catalysts. Here $x = 0, 6, 20,$ and 30 , respectively. (a) Total butenes; (b) 1-butene; (c) *trans*-2-butene; (d) *cis*-2-butene; (e) butane.

hydrogen atoms on small Pd ensembles compared with that on larger Pd ensembles as a result of the enhanced steric effect. The concentration of dissociated hydrogen atoms on small Pd ensembles is likely to be too low for butene hydrogenation, but still sufficient for isomerization. This effect is similar to that of CO additives on a Pd surface [14], and the improvement in alkene selectivity is in line with results observed for single-atom catalysts with high hydrogenation selectivity [5,8,38,39].

4. Conclusions

In this work, we have demonstrated that ultrathin FeO_x coatings can be precisely grown on a $\text{Pd}/\text{Al}_2\text{O}_3$ catalyst using ALD. DRIFT CO chemisorption suggested that FeO_x preferentially decorated the Pd (111) facets, and XPS showed that the Pd NPs became positively charged on addition of FeO_x owing to the strong Pd– FeO_x interaction. In the selective hydrogenation of 1,3-butadiene, we showed that deposition of FeO_x onto the $\text{Pd}/\text{Al}_2\text{O}_3$ catalyst remarkably improved both the hydrogenation activity and butene selectivity. The increase in hydrogenation activity is attributed to electronic effects and the newly generated Pd– FeO_x interface, whereas the enhancement in butene selectivity was mainly induced by a geometric effect, in which large ensembles of Pd surface atoms were divided into smaller ones by FeO_x . This geometric and electronic modulation of Pd catalysts through transition-metal-oxide coatings may open up new opportunities for the improvement of catalysts for other hydrogenation reactions.

Notes

The authors declare no competing financial interest.

References

- [1] B. K. Furlong, J. W. Hightower, T. Y. L. Chan, A. Sarkany, L. Guzzi, *Appl. Catal. A*, **1994**, 117, 41–51.
- [2] J. Goetz, M. A. Volpe, R. Touroude, *J. Catal.*, **1996**, 164, 369–377.
- [3] A. Sarkany, *Appl. Catal. A*, **1998**, 175, 245–253.

- [4] G. G. Cervantes, F. J. C. S. Aires, J. C. Bertolini, *J. Catal.*, **2003**, 214, 26–32.
- [5] D. Yardimci, P. Serna, B. C. Gates, *ACS Catal.*, **2012**, 2, 2100–2113.
- [6] W. D. Bu, L. Zhao, Z. C. Zhang, X. Zhang, J. S. Gao, C. M. Xu, *Appl. Surf. Sci.*, **2014**, 289, 6–13.
- [7] H. Yi, H. Y. Du, Y. L. Hu, H. Yan, H. L. Jiang, J. L. Lu, *ACS Catal.*, **2015**, 5, 2735–2739.
- [8] H. Yan, H. Cheng, H. Yi, Y. Lin, T. Yao, C. L. Wang, J. J. Li, S. Q. Wei, J. L. Lu, *J. Am. Chem. Soc.*, **2015**, 137, 10484–10487.
- [9] R. J. Hou, M. D. Porosoff, J. G. Chen, T. F. Wang, *Appl. Catal. A*, **2015**, 490, 17–23.
- [10] N. El Kolli, L. Delannoy, C. Louis, *J. Catal.*, **2013**, 297, 79–92.
- [11] K. Pattamakomsan, E. Ehret, F. Morfin, P. Gelin, Y. Jugnet, S. Prakash, J. C. Bertolini, J. Panpranot, F. J. C. S. Aires, *Catal. Today*, **2011**, 164, 28–33.
- [12] K. Pattamakomsan, K. Suriye, S. Dokjampa, N. Mongkolsiri, P. Prasertdam, J. Panpranot, *Catal. Commun.*, **2010**, 11, 311–316.
- [13] A. Hugon, L. Delannoy, J. M. Krafft, C. Louis, *J. Phys. Chem. C*, **2010**, 114, 10823–10835.
- [14] J. Silvestre-Albero, G. Rupprechter, H. J. Freund, *J. Catal.*, **2005**, 235, 52–59.
- [15] D. C. Lee, J. H. Kim, W. J. Kim, J. H. Kang, S. H. Moon, *Appl. Catal. A*, **2003**, 244, 83–91.
- [16] A. Sarkany, *J. Catal.*, **1998**, 180, 149–152.
- [17] E. M. Crabb, R. Marshall, *Appl. Catal. A*, **2001**, 217, 41–53.
- [18] F. R. Lucci, M. D. Marcinkowski, E. C. H. Sykes, J. L. Liu, M. Yang, M. Flytzani-Stephanopoulos, L. F. Allard, *Nat. Commun.*, **2015**, 6, 8550.
- [19] R. J. Hou, W. T. Ye, M. D. Porosoff, J. G. G. Chen, T. F. Wang, *J. Catal.*, **2014**, 316, 1–10.
- [20] L. B. Ding, H. Yi, W. H. Zhang, R. You, T. Cao, J. L. Yang, J. L. Lu, W. X. Huang, *ACS Catal.*, **2016**, 3700–3707.
- [21] J. H. Kang, E. W. Shin, W. J. Kim, J. D. Park, S. H. Moon, *Catal. Today*, **2000**, 63, 183–188.
- [22] J. L. Lu, B. S. Fu, M. C. Kung, G. M. Xiao, J. W. Elam, H. H. Kung, P. C. Stair, *Science*, **2012**, 335, 1205–1208.
- [23] H. W. Wang, C. L. Wang, H. Yan, H. Yi, J. L. Lu, *J. Catal.*, **2015**, 324, 59–68.
- [24] H. Feng, J. Lu, P. C. Stair, J. W. Elam, *Catal. Lett.*, **2011**, 141, 512–517.
- [25] J. L. Lu, B. Liu, N. P. Guisinger, P. C. Stair, J. P. Greeley, J. W. Elam, *Chem. Mater.*, **2014**, 26, 6752–6761.

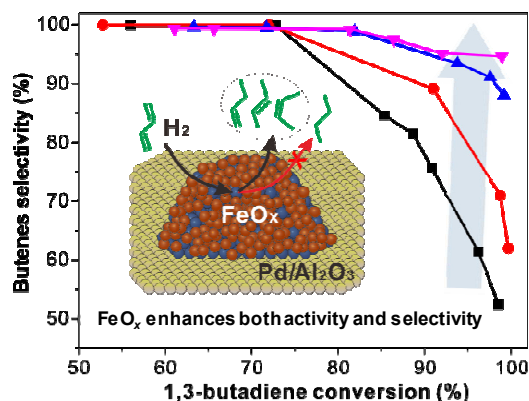
Graphical Abstract

Chin. J. Catal., 2017, 38: 1581–1587 doi: 10.1016/S1872-2067(17)62768-2

Coating $\text{Pd}/\text{Al}_2\text{O}_3$ catalysts with FeO_x enhances both activity and selectivity in 1,3-butadiene hydrogenation

Hong Yi, Yujia Xia, Huan Yan, Junling Lu*
University of Science and Technology of China

Deposition of FeO_x onto $\text{Pd}/\text{Al}_2\text{O}_3$ catalyst can remarkably improve both hydrogenation activity and butenes selectivity through the electronic effect and geometric effect, respectively.



- [26] J. L. Lu, J. W. Elam, P. C. Stair, *Surf. Sci. Rep.*, **2016**, 71, 410–472.
- [27] T. Lear, R. Marshall, J. A. Lopez-Sanchez, S. D. Jackson, T. M. Klapotke, M. Baumer, G. Rupprechter, H. J. Freund, D. Lennon, *J. Chem. Phys.*, **2005**, 123, 174706/1–174706/13.
- [28] M. M. Wei, Q. Fu, A. Y. Dong, Z. J. Wang, X. H. Bao, *Top. Catal.*, **2014**, 57, 890–898.
- [29] A. P. Grosvenor, B. A. Kobe, M. C. Biesinger, N. S. McIntyre, *Surf. Interface Anal.*, **2004**, 36, 1564–1574.
- [30] M. O. Nutt, K. N. Heck, P. Alvarez, M. S. Wong, *Appl. Catal. B*, **2006**, 69, 115–125.
- [31] Y. S. Bi, L. Chen, G. X. Lu, *J. Mol. Catal. A*, **2007**, 266, 173–179.
- [32] N. S. Babu, N. Lingaiah, J. V. Kumar, P. S. S. Prasad, *Appl. Catal. A*, **2009**, 367, 70–76.
- [33] J. A. Rodriguez, P. Liu, D. J. Stacchiola, S. D. Senanayake, M. G. White, J. G. G. Chen, *ACS Catal.*, **2015**, 5, 6696–6706.
- [34] J. Y. Park, L. R. Baker, G. A. Somorjai, *Chem. Rev.*, **2015**, 115, 2781–2817.
- [35] E. Gross, G. A. Somorjai, *Top. Catal.*, **2013**, 56, 1049–1058.
- [36] B. Zhang, Y. Chen, J. W. Li, E. Pippel, H. M. Yang, Z. Gao, Y. Qin, *ACS Catal.*, **2015**, 5, 5567–5573.
- [37] R. Ohnishi, H. Suzuki, M. Ichikawa, *Catal. Lett.*, **1995**, 33, 341–348.
- [38] Z. P. Liu, C. M. Wang, K. N. Fan, *Angew. Chem. Int. Ed.*, **2006**, 45, 6865–6868.
- [39] G. Vile, D. Albani, M. Nachttegaal, Z. P. Chen, D. Dontsova, M. Antonietti, N. Lopez, J. Perez-Ramirez, *Angew. Chem. Int. Ed.*, **2015**, 54, 11265–11269.

通过FeO_x修饰Pd/Al₂O₃催化剂提高催化1,3-丁二烯加氢活性和选择性

易 洪, 夏玉佳, 严 欢, 路军岭*

中国科学技术大学化学物理系, 微尺度物质科学国家实验室(筹), 能量转换材料中国科学院重点实验室, 能源材料化学协同创新中心, 安徽合肥230026

摘要: 石油裂解制备的烯烃流中通常含有 ~1% 二烯烃或者炔烃, 其含量必须降低到 10 ppm 以下以避免其对下游聚合催化剂的毒化作用。对这些副产物选择性加氢生成单烯烃是降低其含量最有前景的方法。Pd 基催化剂具有高的加氢活性和选择性, 是目前最为常用的加氢催化剂, 但是它也存在高转化率下选择性较低和容易因积碳而失活的问题。合成 Pd 基双金属催化剂和对 Pd 催化剂进行氧化物包裹是目前最为常用的方法, 但是这两种方法往往在提高选择性的同时, 降低了 Pd 催化剂的加氢活性。本文利用原子层沉积 (ALD) FeO_x 修饰 Pd/Al₂O₃ 催化剂, 在提高 Pd 催化剂选择性的同时, 1,3-丁二烯选择性加氢活性也得到提高。

表征结果发现, 该样品中 Pd 负载量为 1%, Fe 负载量则随着原子层沉积 FeO_x 周期增加而逐渐增加; 催化剂中 Pd 颗粒大小约为 7 nm, 其表面并未观察到 FeO_x 覆盖层; Pd, Fe 元素分布表明 FeO_x 在 Pd 颗粒表面生长。CO 红外漫反射光谱也发现, 随着 ALD FeO_x 周期的增加, CO 在 Pd 颗粒表面的吸附特征峰强度逐渐降低, 表明 FeO_x 逐渐覆盖 Pd 颗粒表面; 与此同时, 随着 FeO_x 包裹周期的增加, CO 吸附在 Pd(111) 面的特征吸收峰相对于其吸附在边角位的特征峰, 降低得更为明显。这表明 FeO_x 优先覆盖 Pd(111) 面, 而选择性地将 Pd 低配位点暴露, 与 ALD Al₂O₃ 包裹 Pd 颗粒的结果恰恰相反。X 射线光电子能谱分析表明, 在所有催化剂中 Fe 均以 +3 价形式存在; 同时, 因为 Pd-FeO_x 间存在强相互作用, 所以随着 FeO_x 包裹周期的增加, 金属态 Pd 逐渐向高结合能方向移动, 使表面 Pd 处于缺电子状态。

随后, 我们对不同 FeO_x 周期包裹 Pd 催化剂进行了 1,3-丁二烯加氢活性测试。在 25 °C 时 Pd/Al₂O₃ 催化 1,3-丁二烯转化率为 6.7%; 随着温度升高, 转化率逐渐上升, 至 43 °C 时达 100%。相反, 在 26 °C 时, 30Fe/Pd/Al₂O₃ 对 1,3-丁二烯的转化率为 45%, 远高于 Pd/Al₂O₃ 催化剂; 这可能是因为缺电子的 Pd 或 Pd-FeO_x 界面存在所致。Pd/Al₂O₃ 催化剂在较低的转化率 (<75%) 下, 1-丁烯、反式-2-丁烯和顺式-2-丁烯选择性分别为 74%, 20% 和 6%; 随着转化率的增加 (75%~90%), 1-丁烯选择性急剧下降, 丁烷选择性快速上升, 反/顺-2-丁烯选择性也略有增加, 表明此时次级反应 1-丁烯加氢占主导, 同时伴随着 1-丁烯异构化反应; 当转化率继续增加 (>90%), 1-丁烯, 反/顺-2-丁烯加氢生成丁烷为主要反应, 此时丁烷选择性急剧上升, 至转化率为 99% 时, 丁烯选择性仅为 52%。而当 Pd 催化剂表面存在 FeO_x 时, 丁烯选择性随着 FeO_x 周期增加而逐渐增加, 尤其是在较高转化率下 (>75%); 对于 30Fe/Pd/Al₂O₃ 催化剂, 转化率为 99% 时, 丁烯选择性高达 95%。这主要是因为高转化率下, FeO_x 将 Pd 颗粒表面分割成较小的 Pd 团簇, 降低了 Pd 颗粒表面吸附氢气浓度, 抑制了丁烯加氢反应, 而次级反应 1-丁烯异构化占主导, 使得丁烯选择性不变。

关键词: 钯催化剂; 原子层沉积; 加氢; 1,3-丁二烯; 选择性; 活性; 强金属载体相互作用

收稿日期: 2016-11-26. 接受日期: 2016-12-30. 出版日期: 2017-09-05.

*通讯联系人. 电话: (0551)63600359; 电子信箱: junling@ustc.edu.cn

基金来源: 青年千人计划; 国家自然科学基金 (21673215, 51402283, 21473169); 中央高校基本科研业务费专项资金资助 (WK2060030017); 中国科技大学科研启动基金。

本文的英文电子版由 Elsevier 出版社在 ScienceDirect 上出版 (<http://www.sciencedirect.com/science/journal/18722067>).